

## Supporting Information

### **Highly Boosted Gas Diffusion for Enhanced Electrocatalytic Reduction of N<sub>2</sub> to NH<sub>3</sub> on 3D Hollow Co-MoS<sub>2</sub> Nanostructures**

Libin Zeng<sup>†,‡</sup>, Xinyong Li<sup>†,‡</sup>, Shuai Chen<sup>†</sup>, Jiali Wen<sup>†</sup>, Farnood Rahmati<sup>†</sup>, Joshua van der Zalm<sup>†</sup>, Aicheng Chen<sup>\*†</sup>

<sup>†</sup> Electrochemical Technology Center, Department of Chemistry, University of Guelph, 50 Stone Road East, Guelph, ON N1G 2W1, Canada

<sup>‡</sup> State Key Laboratory of Fine Chemicals, Key Laboratory of Industrial Ecology and Environmental Engineering (MOE), School of Environmental Science and Technology, Dalian University of Technology, Dalian 116024, China

## Experimental Section

### Chemicals

Cobalt nitrate hexahydrate ( $\text{Co}(\text{NO}_3)_2 \cdot 6\text{H}_2\text{O}$ ), cetyltrimethylammonium bromide (CTAB), 2-methylimidazole ( $\text{CH}_3\text{C}_3\text{H}_2\text{N}_2\text{H}$ ), sodium citrate ( $\text{CH}_3\text{COONa}$ ), potassium hexacyanoferrate (III) ( $\text{K}_4\text{Fe}(\text{CN})_6$ ), sodium sulfate ( $\text{Na}_2\text{SO}_4$ ), sodium hydroxide ( $\text{NaOH}$ ), sodium salicylate ( $\text{C}_7\text{H}_5\text{O}_3\text{Na}$ ), sodium hypochlorite ( $\text{NaClO}$ ), sodium nitroferricyanide (III) ( $\text{C}_5\text{FeN}_6\text{Na}_2\text{O}$ ), and ammonium chloride ( $\text{NH}_4\text{Cl}$ ) were purchased from Sigma-Aldrich Chemical Reagent Co. Ltd. Nafion (1 wt.%) solution, hydrogen peroxide ( $\text{H}_2\text{O}_2$ ), and ethanol were purchased from Aladdin Ltd. Ammonium tetrathiomolybdate ( $(\text{NH}_4)_2\text{MoS}_4$ ) was purchased from New Jersey, USA. All reagents were of analytical grade and used without further purification. Further, a cation exchange membrane (CEM) was purchased from the DuPont Company. Deionized water (18.2 M $\Omega$  cm) was used in all experiments.

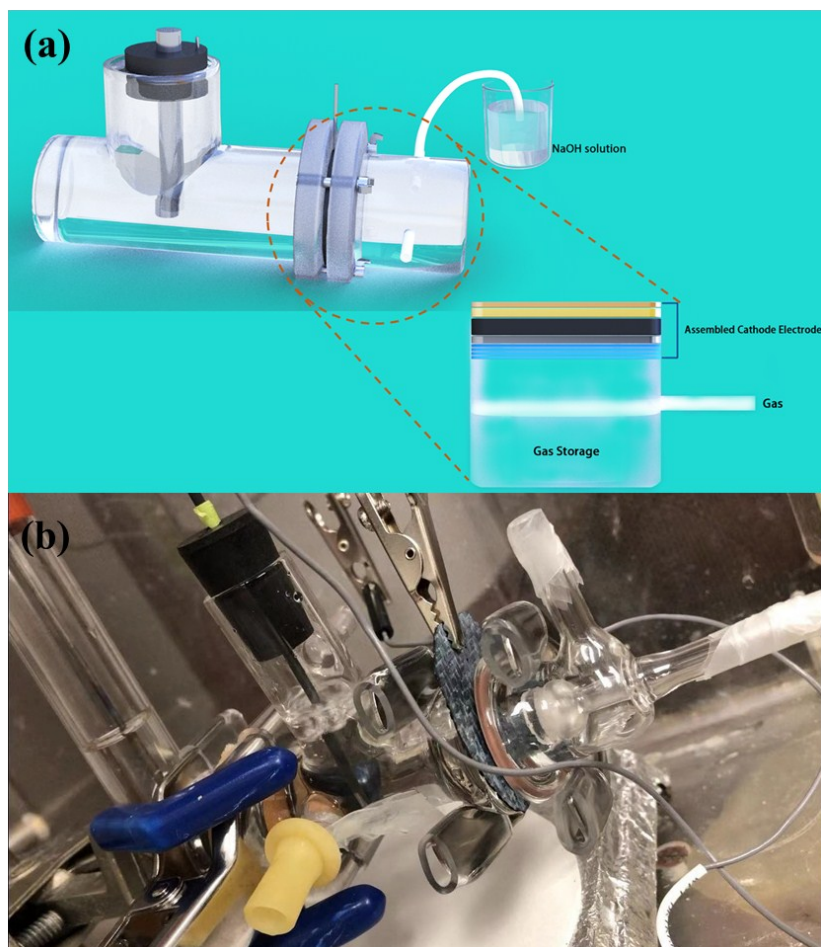
### Characterization of nanomaterials

A field-emission scanning electron microscopy (FE-SEM) (Hitachi, USA) and high-resolution transmission electron microscopy (HRTEM) (FEI Tecnai F30 electron microscope, using a 200 kV accelerating voltage) were used to characterize the morphology and crystallinity of the as-prepared Co-MoS<sub>2</sub> catalysts. X-ray diffraction (XRD) with a diffractometer with Cu  $K\alpha$  radiation (PW1050-3710, Japan, source light at the wavelength ( $\lambda$ ) of 0.1541 nm) was employed to investigate the crystalline structure of the as-prepared catalysts. The chemical compositions and oxidation states of

the as-prepared Co@MoS<sub>2</sub> catalysts were investigated via X-ray photoelectron spectroscopy (XPS) (Thermo Scientific K- $\alpha$  XPS spectrometer, USA). The specific surface area and pore size distribution were elucidated by nitrogen adsorption/desorption isotherms on a Quantachrome instrument (NOVA 4200e, USA). Raman spectra were recorded at 532 nm using a Raman spectrophotometer (Renishaw Canada Ltd.).

**Table S1.** Comparison of MoS<sub>2</sub>-based catalysts for the electrochemical synthesis of ammonia.

| Catalysts                                | Conditions                                  | Faradaic Efficiency (%) / | Ammonia Yield  | Ref.      |
|--|---|---------------------------|--|-----------|
|  |   | Bias (V vs. RHE)          | ( $\mu\text{g h}^{-1} \text{mg}^{-1}_{\text{cat.}}$ )/Bias |           |
| MoS <sub>2</sub> nanosheets              | 25°C, 0.1 M Na <sub>2</sub> SO <sub>4</sub> | 1.17/-0.5                 | 13.09/-0.5   | 1         |
| Defect-rich MoS <sub>2</sub> nanoflowers | 25°C, 0.1 M Na <sub>2</sub> SO <sub>4</sub> | 8.34/-0.4                 | 29.28/-0.4   | 2         |
| S@MoS <sub>2</sub> nanosheets            | 25°C, 0.1 M Li <sub>2</sub> SO <sub>4</sub> | 9.81/-0.2                 | 43.4/-0.2  | 3         |
| N@MoS <sub>2</sub> nanoflowers           | 25°C, 0.1 M Na <sub>2</sub> SO <sub>4</sub> | 9.14/-0.3                 | 69.82/-0.3   | 4         |
| Au@MoS <sub>2</sub> nanosheets           | 20°C, 0.1 M KOH                             | 9.7/-0.3                  | 25.00/-0.3   | 5         |
| Ru@MoS <sub>2</sub>                      | 50°C, 0.1 M Na <sub>2</sub> SO <sub>4</sub> | 17.6/-0.15                | 6.98/-0.15   | 6         |
| MoS <sub>2</sub> @rGO                    | 20°C, 0.1 M LiClO <sub>4</sub>              | 4.56/-0.45                | 24.82/-0.45  | 7         |
| Co-MoS <sub>2</sub> (20:1)               | 20°C, 0.1 M Na <sub>2</sub> SO <sub>4</sub> | 11.21/-0.4                | 129.93/-0.4  | This work |



**Scheme S1.** (a) Schematic diagram of the constructed two-chamber cell used for the NRR; (b) the original image of the electrochemical cell system.

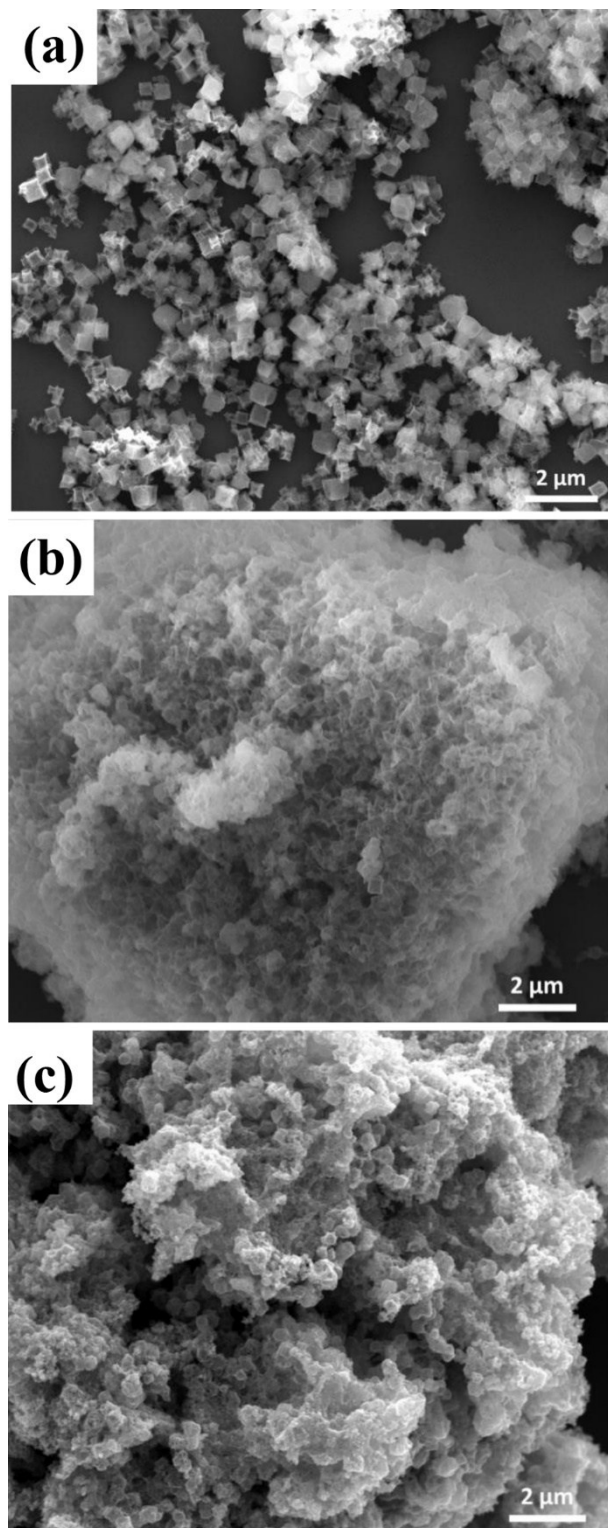


**Figure S1.** SEM images of Co-MoS<sub>2</sub> catalysts: (a) Co-MoS<sub>2</sub> (20:1), (b) Co-MoS<sub>2</sub> (10:1), and (c) Co-MoS<sub>2</sub> (1:1) samples.

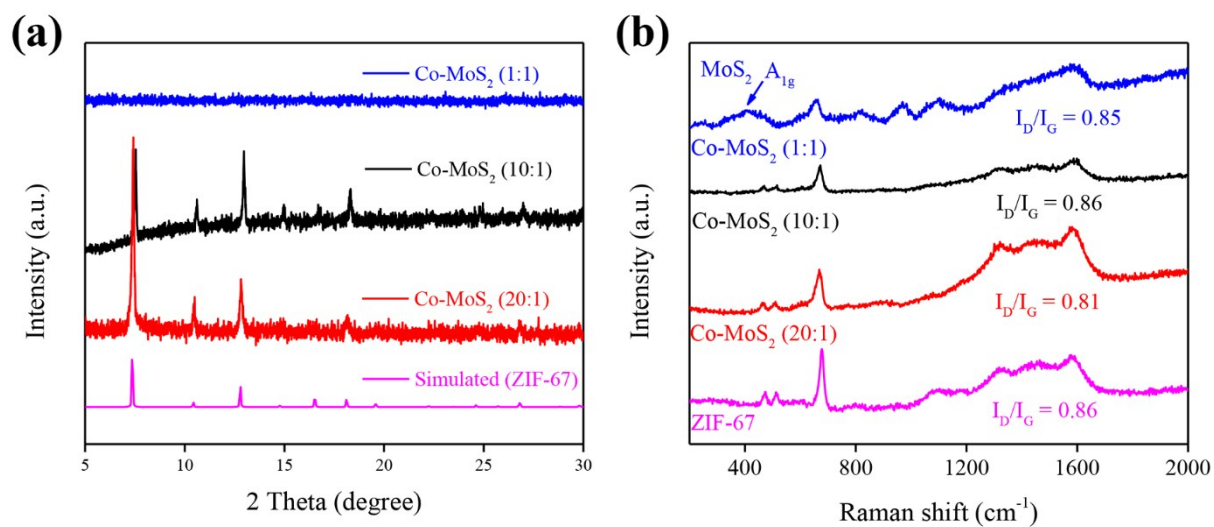


**Figure S2.** (a) XRD spectra of Co-MoS<sub>2</sub> (20:1), Co-MoS<sub>2</sub> (10:1), Co-MoS<sub>2</sub> (1:1) and simulated pattern of ZIF-67 structure samples; (b) the corresponding Raman spectra with the excitation at 532 nm.

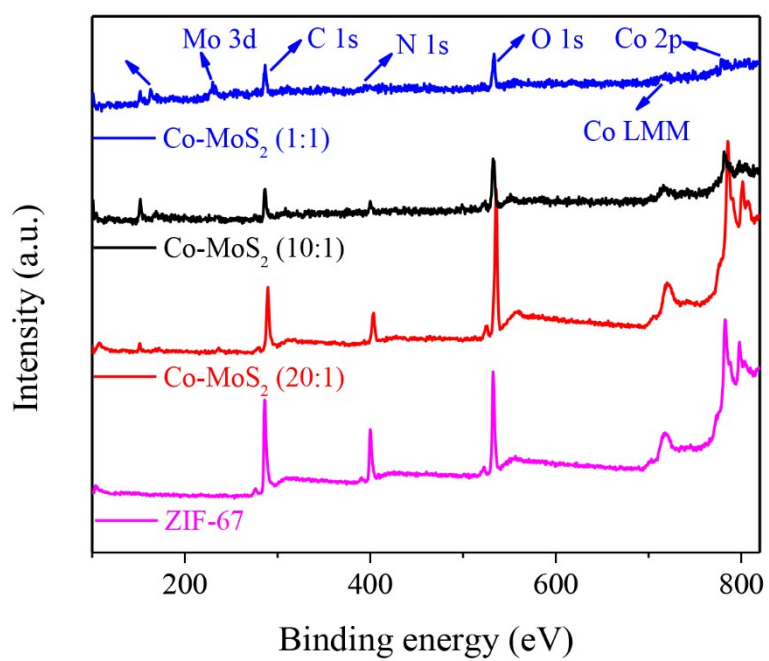


**Figure S3.** XPS surveys of the as-prepared ZIF-67 and the Co-MoS<sub>2</sub> catalysts.



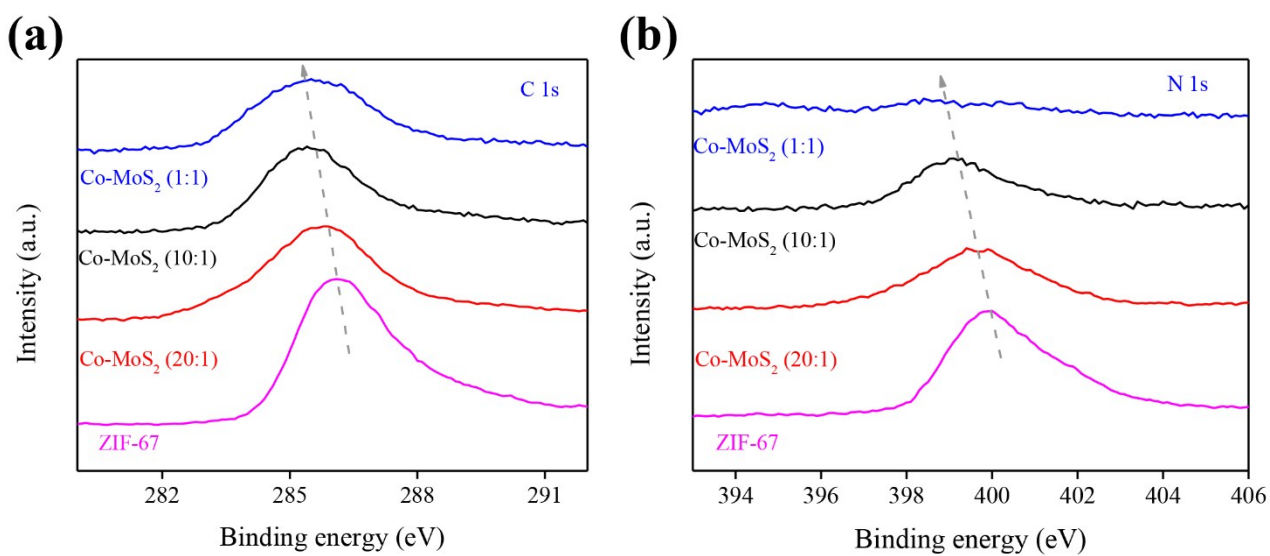


**Figure S4.** High-resolution XPS spectra of C 1s (a) and N 1s (b) of ZIF-67 and the different Co-coped MoS<sub>2</sub> samples, respectively.

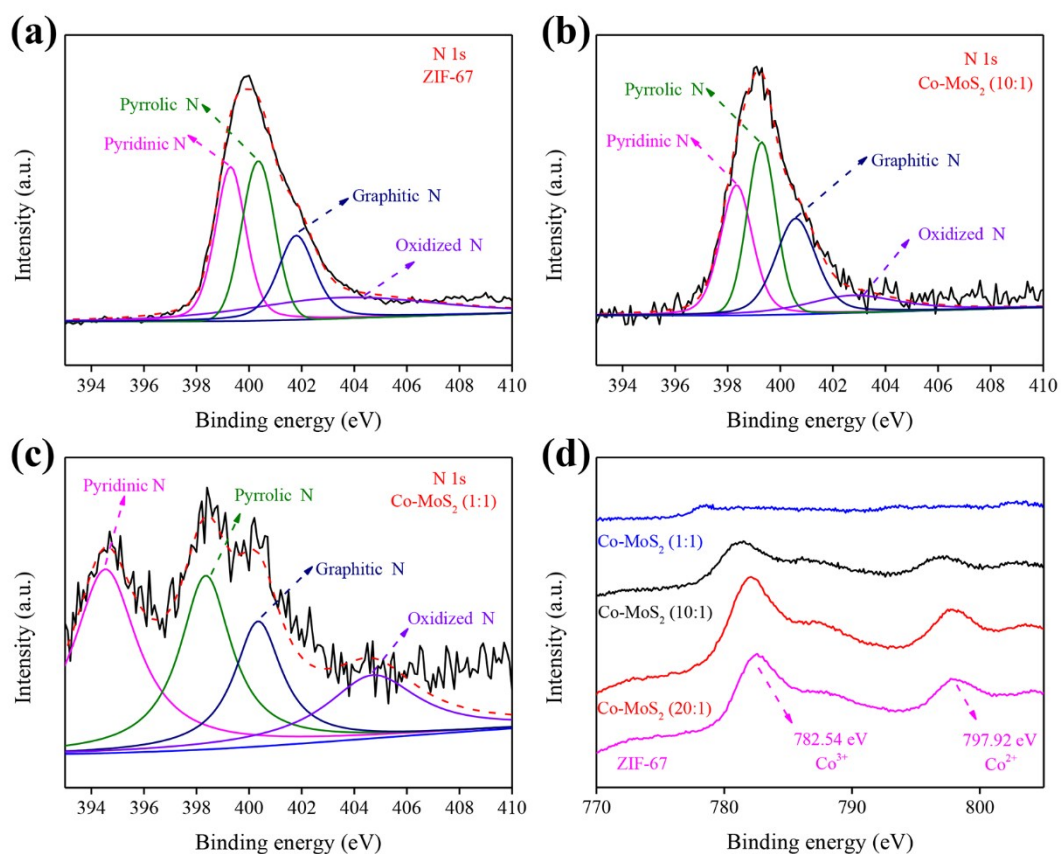


**Figure S5.** High-resolution XPS spectra and the fitted N 1s spectra of (a) ZIF-67, (b) Co-MoS<sub>2</sub> (10:1) and (c) Co-MoS<sub>2</sub> (1:1) catalysts; (d) high-resolution XPS spectra of Co 2p of ZIF-67 and the Co-doped MoS<sub>2</sub> samples.

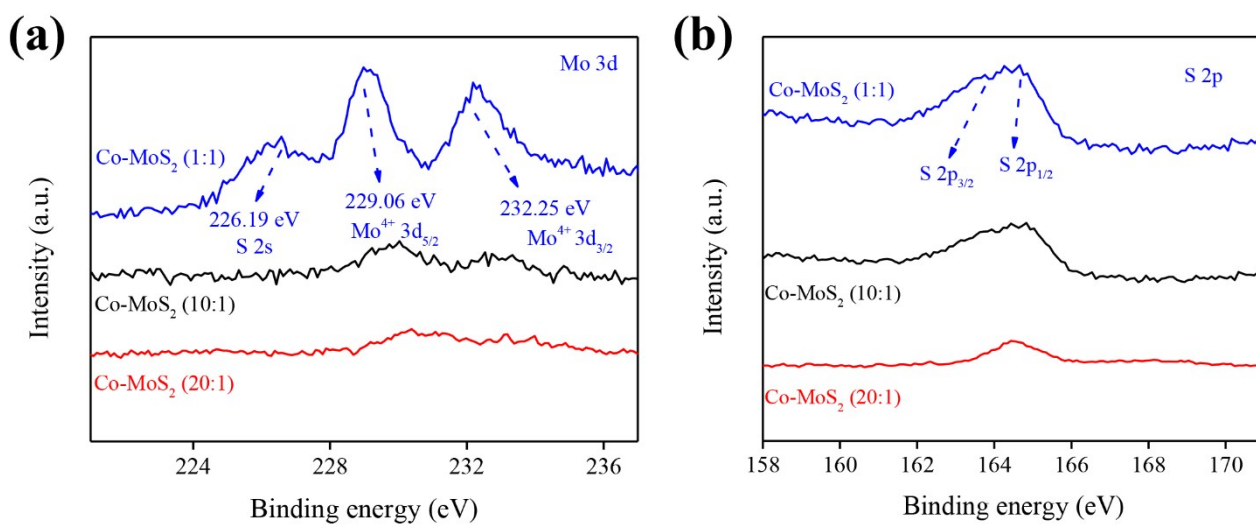


**Figure S6.** High-resolution XPS spectra of Mo 3d (a) and S 2p (b) of the Co-doped MoS<sub>2</sub> samples.

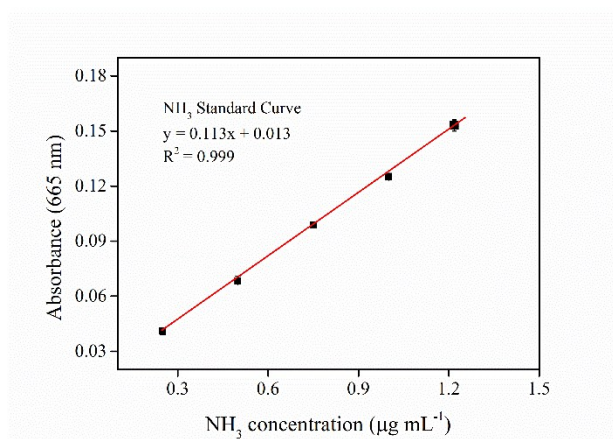


**Figure S7.** Calibration curve used for the estimation of NH<sub>3</sub> via NH<sub>4</sub><sup>+</sup> ion concentration.

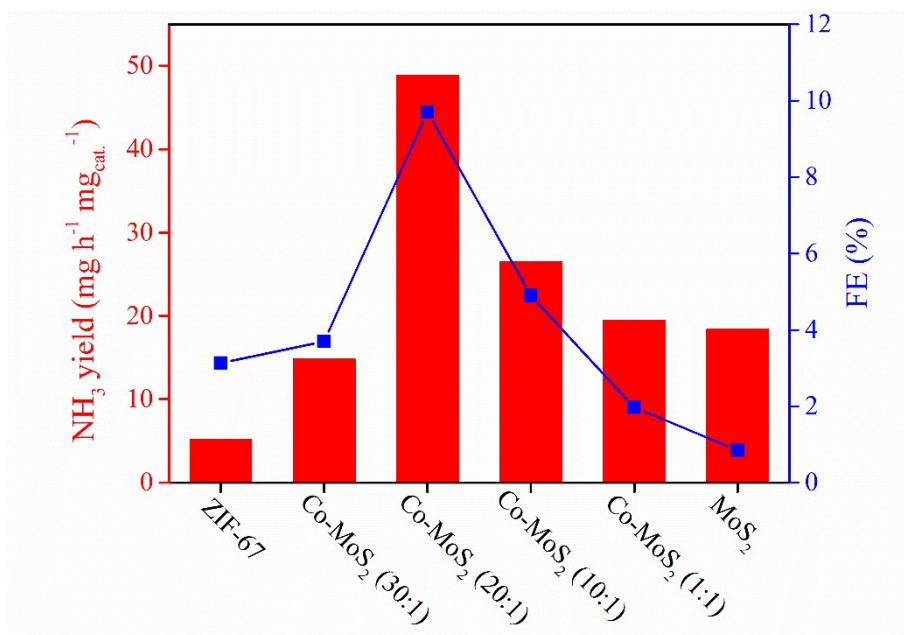


**Figure S8.** NH<sub>3</sub> yields and corresponding FEs of the different catalysts at -0.4 V vs. RHE.

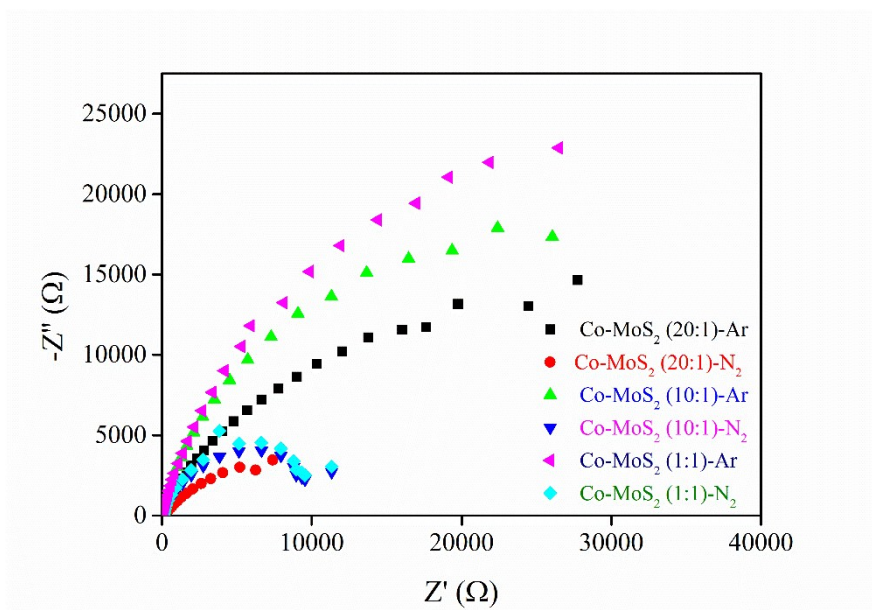


**Figure S9.** Electrochemical impedance spectra of the different Co-MoS<sub>2</sub> catalysts recorded under the Ar-/N<sub>2</sub>-saturated conditions.

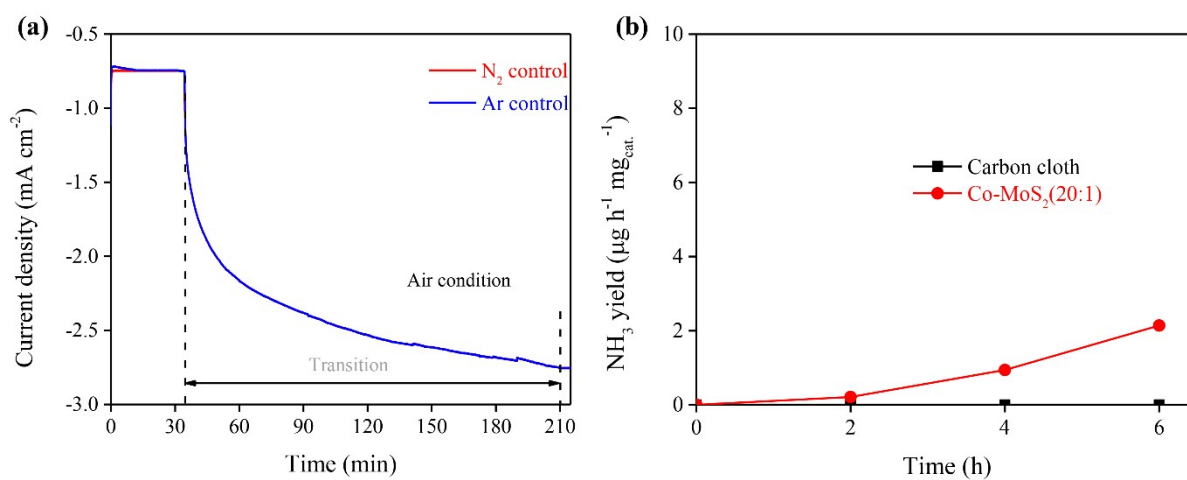


**Figure S10.** (a) Chronoamperometry curves of the carbon black under N<sub>2</sub> and Ar (30 min), and the corresponding air transition stage (-0.4 V vs RHE); (b) NH<sub>3</sub> yield over carbon black and Co-MoS<sub>2</sub>(20:1) catalyst at the potential of -0.4 V vs RHE, respectively, where Ar gas was purged through the solution for 30 min and then was stopped.

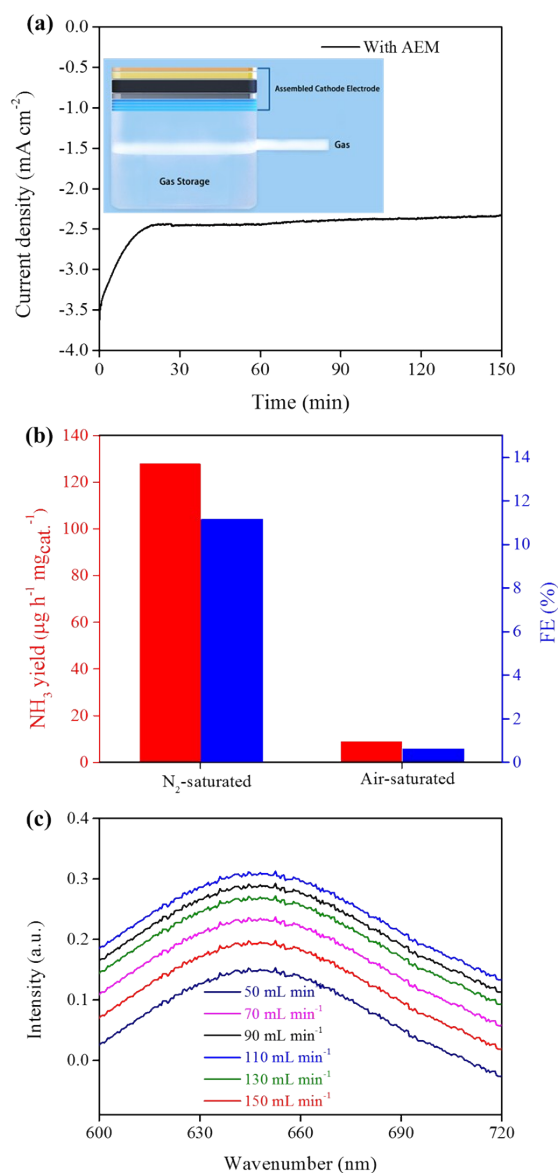


**Figure S11.** (a) Chronoamperometric curves of the Co-MoS<sub>2</sub> catalyst during the gas transition with CEM at the applied electrode potential of -0.4 V vs. RHE; (b) corresponding NH<sub>3</sub> yields and FEs at selected positions; (c) UV-vis spectra of the NRR under different N<sub>2</sub> flow rate.



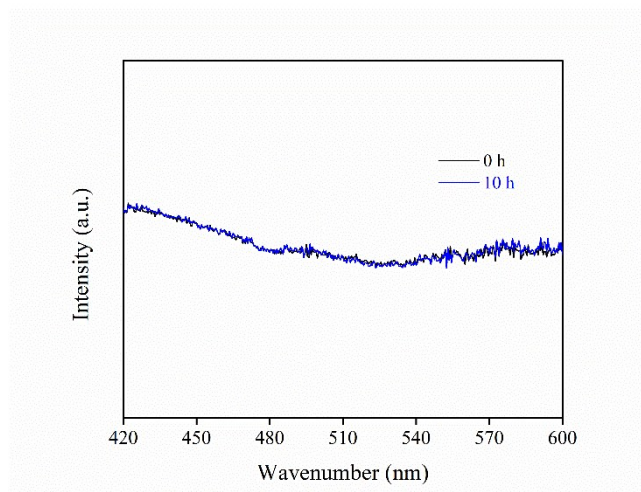


**Figure S12.** UV-Vis spectra of the NRR prior to and following the 10-hour electrolysis at -0.4 V vs. RHE with the GDE.

## References

1. L. Zhang, X. Ji, X. Ren, Y. Ma, X. Shi, Z. Tian, A. M. Asiri, L. Chen, B. Tang and X. Sun, *Adv. Mater.*, 2018, **30**, 1800191.
2. X. Li, T. Li, Y. Ma, Q. Wei, W. Qiu, H. Guo, X. Shi, P. Zhang, A. M. Asiri, L. Chen, B. Tang and X. Sun, *Adv. Energy Mater.*, 2018, **8**, 1801357.
3. Y. Liu, M. Han, Q. Xiong, S. Zhang, C. Zhao, W. Gong, G. Wang, H. Zhang and H. Zhao, *Adv. Energy Mater.*, 2019, **9**, 1803935.
4. L. Zeng, S. Chen, J. van der Zalm, X. Li and A. Chen, *Chem. Commun.*, 2019, **55**, 7386-7389.
5. Y. Zhou, X. Yu, X. Wang, C. Chen, S. Wang and J. Zhang, *Electrochim. Acta*, 2019, **317**, 34-41.
6. B. H. R. Suryanto, D. Wang, L. M. Azofra, M. Harb, L. Cavallo, R. Jalili, D. R. G. Mitchell, M. Chatti and D. R. MacFarlane, *ACS Energy Lett.*, 2018, **4**, 430-435.
7. X. Li, X. Ren, X. Liu, J. Zhao, X. Sun, Y. Zhang, X. Kuang, T. Yan, Q. Wei and D. Wu, *J. Mater. Chem. A*, 2019, **7**, 2524-2528.